Reexamination of the excited states of ^{12}C

M. Freer,[1] I. Boztosun,[2,*] C. A. Bremner,[2] S. P. G. Chappell,[2] R. L. Cowin,[3] G. K. Dillon,[3] B. R. Fulton,[3] B. J. Greenhalgh,[3] T. Munoz-Britton,[1] M. P. Nicoli,[1] W. D. M. Rae,[2] S. M. Singer,[1] N. Sparks,[1] D. L. Watson,[3] and D. C. Weisser[4]

[1]*School of Physics and Astronomy, University of Birmingham, Edgbaston, Birmingham B15 2TT, United Kingdom*

[2]*Nuclear and Astrophysics Laboratory, University of Oxford, Keble Road, Oxford OX1 3RH, United Kingdom*

[3]*Department of Physics, University of York, Heslington, York YO10 5DD, United Kingdom*

[4]*Department of Nuclear Physics, The Australian National University, Canberra ACT 0200, Australia*

(Received 6 June 2007; revised manuscript received 31 July 2007; published 24 September 2007)

An analysis of the ^{12}C(^{12}C, 3α)^{12}C reaction was made at beam energies between 82 and 106 MeV. Decays to both the ground state and the excited states of ^{8}Be were isolated, allowing states of different characters to be identified. In particular, evidence was found for a previously observed state at 11.16 MeV. An analysis of the angular distributions of the unnatural parity states at 11.83 and 13.35 MeV, previously assigned $J^{\pi} = 2^{-}$, calls into question the validity of these assignments, suggesting that at least one of the states may correspond to $J^{\pi} = 4^{-}$. Evidence is also found for 1^{-} and 3^{-} strengths associated with broad states between 11 and 14 MeV.

DOI: 10.1103/PhysRevC.76.034320 PACS number(s): 25.70.Ef, 25.70.Mn, 27.20.+n

I. INTRODUCTION

The formation of the ^{12}C nucleus is rather crucial in nucleosynthesis because it provides both the gateway to heavier elements and also the key ingredient in organic molecules. Surprisingly, the structure above the first excited state remains something of a mystery. The nature of the second excited state at 7.65 MeV, 0^{+}, the famous Hoyle state (through which ^{12}C is synthesized), remains a subject of great debate [1–5]. It is believed to have a large radius that perhaps gives rise to a Bose gas of α particles. Such a state is certainly not described within the shell model [6]. However, a clear candidate for a 2^{+} excitation of this state has remained elusive, though some possibilities exist [7,8]. The identification of the 2^{+} excitation of the Hoyle state remains one of the most important challenges of the subject.

The next state lies at 9.64 MeV, 3^{-}. This has been associated with a $K^{\pi} = 3^{-}$ cluster structure [9]. If it is a cluster state, then it should give rise to the rotational sequence 3^{-}, 4^{-}, 5^{-}, ... However, no reasonable candidate for the 4^{-} state has yet been observed. On the other hand, the shell model does predict a 3^{-} state at about the correct energy. The resolution of the rotational characteristics is crucial in determining the properties of this state. Similarly, the 10.84 MeV 1^{-} state is associated with a cluster structure [9], the rotational characteristics of which have yet to be pinned down. In this region of great interest, not least from the astrophysical perspective, it is remarkable that so little is really understood about this very important nucleus.

In this article we examine some of the spin assignments of excited states above the Hoyle state with a view of verifying some of the *established* experimental properties. This has been accomplished through an analysis of the α-decaying ^{12}C excited states populated through the ^{12}C(^{12}C, 3α)^{12}C reaction.

II. EXPERIMENTAL DETAILS

The present analysis is based on measurements that were performed at the Australian National University (ANU). The experiment was conducted using the Charissa strip detector array located in the MEGHA chamber [10]. The array was composed of eight 500 μm, (50 × 50) mm Si strip detectors. These covered an angular range of $\theta_{\mathrm{lab}} = 5$ to 60°, and an azimuthal angular range $\Delta\phi \approx 100°$ degrees each side of the beam axis, as shown in Fig. 1 of Ref. [11]. Each strip detector was divided into 16 position-sensitive strips, with the position-sensitive axis orientated toward the beam axis. The energy response of the detection system was calibrated using elastic scattering of ^{12}C ions from both ^{197}Au and ^{12}C targets. The combined energy resolution of 16 strips was typically 200 keV (FWHM) and the position resolution was 0.5 mm (FWHM).

^{12}C beam energies of 82, 86, 88, 96, 104, and 106 MeV were used, with intensities of 50 enA. These were incident upon a 60 μg cm^{-2} ^{12}C target foil. The beam energies were obtained using the linear accelerator in conjunction with the pelletron tandem 14UD accelerator.

III. ANALYSIS AND RESULTS

A. Excitation energy spectra

The events selected for the present analysis were those associated with the ^{12}C(^{12}C, 3α)^{12}C reaction, in which one of the ^{12}C nuclei was excited above the α-decay threshold. The detection of all of the four final-state particles allows the unambiguous selection of events connected with the above reaction. In the instance that all of the particles are produced in their ground states, the sum of the final-state kinetic energies is equal to the sum of the beam energy and the reaction Q value (−7.272 MeV). If any of the nuclei are produced in an excited state (in this case it is only possible for the ^{12}C nucleus) then this will correspond to the final-state kinetic energy being reduced by an amount corresponding to the excitation energy of the corresponding state. Figure 1(a) shows the sum of the

*Department of Physics, Erciyes University, 38039 Kayseri, Turkey.

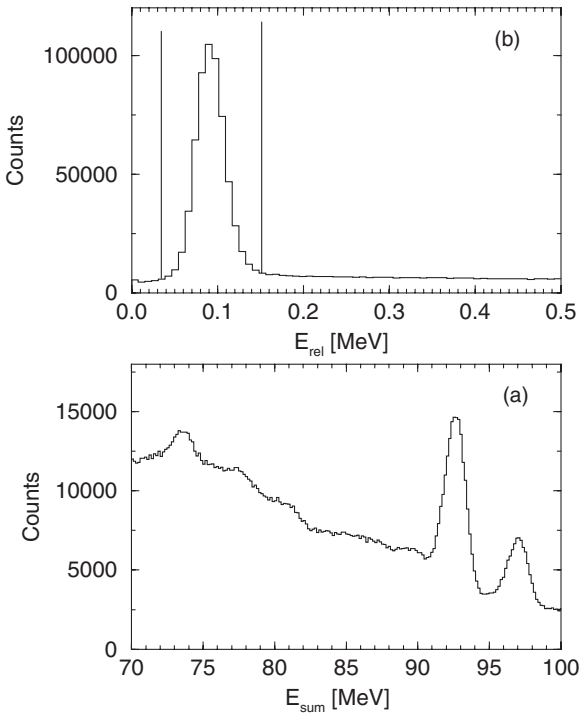

FIG. 1. (a) The summed energies of the four detected particles for the beam energy of 106 MeV. The events between 91 and 99 MeV were selected for analysis. (b) The α-α relative energy spectrum, showing the peak that corresponds to the characteristic decay of the ^{8}Be ground state at $E_{\rm rel} = 93$ keV. The two vertical lines show the region of relative energies that were used to define decays to the ^{8}Be ground state.

kinetic energies of the four final-state particles. The two peaks correspond to the ^{12}C nucleus being formed either in the ground state or in the first excited state (4.44 MeV). Data contained within both of the peaks shown were selected for further analysis.

For the three detected α particles it is possible to reconstruct the excitation energy of the system from which they were formed. In the first instance, the relative energy between pairs of α particles was calculated to determine if they corresponded to the α decay of ^{12}C to the ground state of ^{8}Be. The relative energy was calculated via

$$E_{\rm rel} = \tfrac{1}{2}\mu v_{\rm rel}^2, \qquad (1)$$

where μ is the reduced mass and $v_{\rm rel}$ is the relative velocity of the two α particles in the ^{8}Be center-of-mass frame. The corresponding spectrum is shown in Fig. 1(b). The peak that appears at 93 keV corresponds to the decay of the ^{8}Be ground state to two α particles.

To separate ^{12}C decays to the ground and excited states of ^{8}Be, the ^{12}C excitation energy spectra were produced by demanding that the reconstructed decay energy of any pair of the three α particles coincides with the peak in Fig. 1(b), in which case it is assumed that the decay of ^{12}C proceeds to the ground state of ^{8}Be. If, however, none of the three combinations produces a decay energy that falls within the peak, then the decay is assumed to proceed via the first excited state, $E_x = 2.9$ MeV, 2^+. The resulting ^{12}C excitation energy spectra are shown in Figs. 3 and 4. These ^{12}C excitation energy spectra were calculated using momentum conservation; the momentum of the three α particles was used to deduce that of the parent ^{12}C nucleus. This allows the kinetic energy (KE) of the ^{12}C nucleus to be deduced and, thus, from the difference between the initial KE of the ^{12}C nucleus and that of the α particles the decay Q value can be deduced. Thus, the excitation energy of ^{12}C may be calculated independent of the decay route:

$$E_x(^{12}{\rm C}) = \sum_{i}^{3} E_\alpha(i) - \frac{\sum_i^3 p_\alpha(i)^2}{2m_c} + E_{\rm thresh}. \qquad (2)$$

Here, E_x, $E_{\rm thresh}$, and m_c are the excitation energy, 3α-decay threshold, and the mass of ^{12}C, and $E_\alpha(i)$ and $p_\alpha(i)$ are the energies and momenta of the three α particles.

The experimental excitation energy spectra have been fitted with all of the known states between 7 and 15 MeV [12], which are shown in Fig. 2. The Gaussian widths of the peaks were determined by adding the experimental resolution in quadrature with the known widths. The resolution was found to follow the form $R({\rm FWHM}) = [0.42\sqrt{E_x - E_{\rm thresh}} - 0.14]$ (MeV), where R is the resolution and $E_{\rm thresh}$ is the α-decay threshold. In other words, the only free parameters in the fit are the peak amplitudes and the magnitude of the background contribution to the spectra. The background largely originates from reactions such as ^{12}C(^{12}C, ^{16}O[^{12}C + α])^{8}Be, which cannot be completely removed. Obvious contributions from decays of excited states in ^{16}O have been excluded. However, contributions from broad resonances at high excitation energies almost certainly remain. In the case of the decay to the ^{8}Be ground state a contribution from the broad 10.3 MeV (0^+) state found in, for example, β-decay measurements is

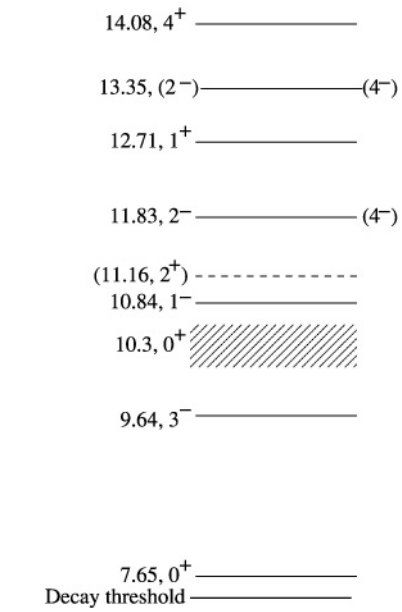

FIG. 2. ^{12}C energy levels above the α-decay threshold. The labels on the right-hand side are those from Ref. [12], and the (4^-) labels indicate the two resonances whose decay properties are found in the present measurements to be consistent with a 4^- assignment.

also included [8]. The parametrization of the peak shape was taken from Ref. [8] and is shown in Fig. 2 of Ref. [8].

In the analysis of the decay to the ^{8}Be ground state, the dominant contributions from narrow resonances come from the 7.65 MeV (0^+), 9.64 MeV (3^-), 10.84 MeV (1^-), and 14.08 MeV (4^+) natural parity states. A further peak was included in the fit corresponding to the unassigned state at 11.16 MeV [12]; there is a negligible contribution from this state to the spectrum. The important states in the decay to ^{8}Be excited states are 9.64 MeV (3^-), 10.84 MeV (1^-), 11.83 MeV (2^-), 12.71 MeV (1^+), 13.35 MeV ([2^-]), and 14.08 MeV (4^+). There appears to be a small but necessary contribution from a state at 11.16 MeV reported in Ref. [12]. As judged from the residuals, the fits to the two spectra include all of the important components from narrow resonances in the present excitation energy region.

The unnatural parity states are clearly evident from their strong contribution to the ^{8}Be* decay channel and absence from decays to the ground state. The branching fractions of the 14.08 MeV state to the ground and excited states of ^{8}Be are calculated to be 17 and 83%, respectively (correcting for the calculated ratio of the detection efficiencies, which is larger for the ground state decay by a factor of 1.46). This is in very good agreement with the measurements of the branching ratio reported in Ref. [13] (83.0±0.4%). Similarly, the percentage decays for the 9.64 MeV 3^- state to the ground and first excited states are found to be 97.2 and 2.7%, respectively.

As noted above, in the decay to the 2.9 MeV excited state in ^{8}Be there is evidence for the previously reported 11.16 MeV state that has been tentatively associated with $J^\pi = 2^+$. The yield in this region cannot be accounted for by the presence of the decay from the 10.84 MeV 1^- state. Only an upper limit of 38% can be determined for the decay of the state at 11.16 MeV to the ground state. The dominant decay branch is to the 2.9 MeV excited state.

There are reasonably strong deviations in the residuals (compared with the magnitudes of the statistical errors) close to the 7.65 and 9.64 MeV peaks in Fig. 3. In part, this represents the fact that the tails of the peak shape, employed in the fit to the data, do not accurately describe the data. It should be noted that due to the fact that the excitation energy spectra are calculated from the responses of 128 individual strips, with slightly differing calibrations, this can lead to a non-Gaussian response. However, there does appear to be an excess of counts beyond that which can be accounted for by such details in the high energy side of the 9.64 MeV peak in Fig. 4 extending up to ~10.4 MeV. This is, of course, very close to the region occupied by the broad 10.3 MeV 0^+ state and may in fact be due to the incorrect description of the resonance shape. However, a similar feature is also seen in the decay of the 9.64 MeV state to the 2.9 MeV ^{8}Be state. Here, tails exceeding the anticipated peak line-shape are observed both at low and at high energy. In this latter spectrum, the contribution from the decay of the 10.3 MeV state is expected to be suppressed because of the centrifugal barrier. It is thus possible that there is a state in this region that has a width which is ~900 keV at an energy close to 9.6 MeV as suggested in Ref. [7]. The analysis of the data in Ref. [7] suggested that such a state might have $J^\pi = 2^+$. The corresponding decay to the broad ^{8}Be 2^+ state

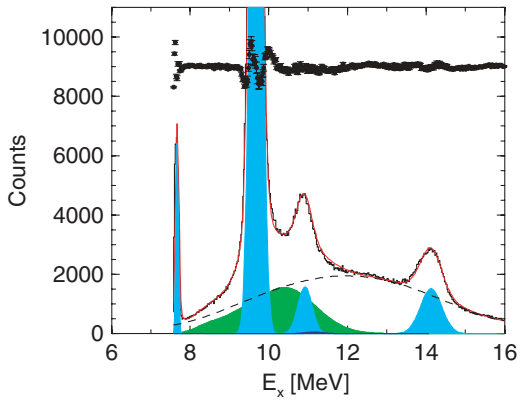

FIG. 3. (Color online) ^{12}C excitation energy spectrum for decays to $\alpha + {}^{8}\mathrm{Be}_{\mathrm{gs}}$. The histogram corresponds to the experimental data, the (red) solid line corresponds to the fit, and the (black) dashed line corresponds to the estimated background. The peaks included in the fit are shown in pale blue, the broad peak at 10.3 MeV (green) is parametrized using a form from Ref. [8], and the very small contribution from a state at 11.16 MeV is shown in darker blue. The residuals of the fit to the data are shown across the top of the spectrum (filled circles).

would have no centrifugal barrier, compared with the finite barrier that appears in the case of the decay of the 9.64 MeV, 3^-, state. As a consequence, the decay of a 2^+ state should decay, on average, to higher ^{8}Be excitations when compared with the decay of the 3^- state. An analysis of the width of the ^{8}Be excited state as a function of ^{12}C excitation energy indicates no significant change in width or centroid. There is no additional high ^{8}Be excitation energy component associated with the presence of a $l = 0$ barrier. In fact, it is observed that the broad component seen in Fig. 4 corresponds to a small amount of leak-through from decays to the ^{8}Be ground state, where the tails of the ground state peak [outside the lines in Fig. 1(b)] are included in the present analysis. These tails are

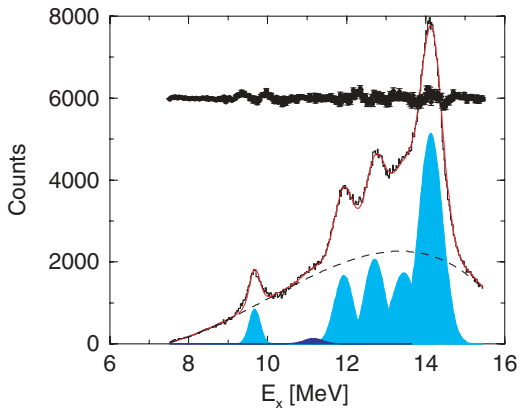

FIG. 4. (Color online) ^{12}C excitation energy spectrum for decays to $\alpha + {}^{8}\mathrm{Be}^*$. The histogram corresponds to the experimental data, the (red) solid line corresponds to the fit, and the (black) dashed line corresponds to the estimated background. The peaks included in the fit are shown in pale blue, and the magnitude of the contribution from a state at 11.16 MeV is shown in darker blue. The residuals of the fit to the data are shown across the top of the spectrum (filled circles).

the components of the decay to the ground state that have the largest deviation from the mean peak energy and it is this which gives the non-Gaussian behavior that is observed for the 3^- peak.

Thus, to summarize, there is in fact no substantial evidence for a 2^+ state close to 9.6 MeV in the present data.

B. Decay correlations

1. *Decays to* ^{8}Be(0^+) *ground state*

Given that both the initial and final states contain exclusively spin zero particles, it is possible to utilize the technique of angular correlations to extract the spins of the observed states [14]. Furthermore, if the decay is into two spin zero particles, e.g., $^8\mathrm{Be}_{gs} + \alpha$, then it is only possible to observe states with natural parity, $\pi = (-1)^J$.

In the present reaction there are two center-of-mass systems: that corresponding to the $^{12}\mathrm{C} + {}^{12}\mathrm{C} \rightarrow {}^{12}\mathrm{C}^* + {}^{12}\mathrm{C}$ inelastic scattering reaction, which may be described in terms of the two angles θ^* and ϕ^*, and the second being the subsequent decay into $^8\mathrm{Be} + {}^4\mathrm{He}$ nuclei, described by the angles ψ and χ (as detailed in Ref. [14]). The angles θ^* and ψ are the polar angles measured with respect to the beam axis and measure the center-of-mass emission angle of the ^{12}C ejectile and the inclination of the $^8\mathrm{Be} + {}^4\mathrm{He}$ relative velocity vector. The angles ϕ^* and χ are the two corresponding azimuthal angles.

Typically, for reactions involving spin zero initial and final-state particles the number of reaction amplitudes is small and the correlations observed between the two angles θ^* and ψ take the form of a sloping ridge pattern. The periodicity of the ridges is described by a Legendre polynomial of the order of the spin of the decaying state, i.e., $P_J(\cos\psi)$. As the dominant orbital angular momenta in the reaction are those corresponding to grazing trajectories, the gradient of the ridges is given by the ratio of the exit channel grazing angular momentum to the spin of the state populated,

$$\frac{\Delta\theta^*}{\Delta\psi} = \frac{J}{l_f} = \frac{J}{l_i - J}, \tag{3}$$

where l_i and l_f are the initial and final state grazing angular momenta. If the "stretched" configuration dominates, which is typically the case for such reactions (see Ref. [14] and references therein), then the entrance and exit channel angular momenta can be related via the expression $l_f = l_i - J$.

The angular correlations therefore provide two signatures of the spin of the decaying ^{12}C state. The periodicity yields a value for J, which should correlate with that extracted from the ridge gradient, assuming l_i is known. In addition, the value of J extracted from the periodicity should provide a consistent value of l_i for all of the correlations. In the present case (which used the beam energies 82–96 MeV) this was found to be close to 23 $\hbar$. The correlation data were projected onto the ψ axis at an angle that is defined by Eq. (3) and this value of l_i. The results of this analysis are shown in Fig. 5. It is observed that the range of angles is larger than 0 to 360° degrees. This is a feature of such correlation analysis where the data that are constrained in the θ^*–ψ plane to lie in the above range,

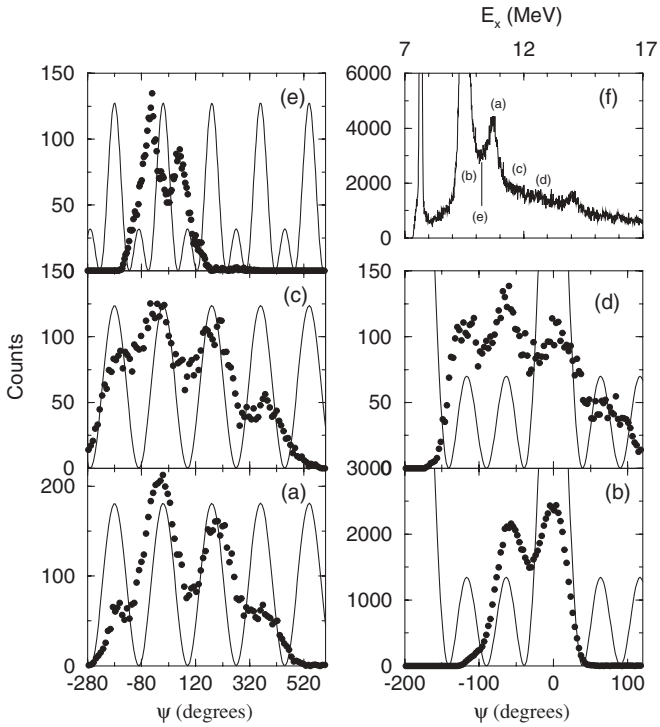

FIG. 5. Angular distributions (circles), panels (a) to (e), for portions of the ^{12}C excitation energy spectrum shown in panel (f). The periodicity of the angular distributions are compared with Legendre polynomials (solid lines). (a) 1^- state at 10.84 MeV compared with a $|P_1(\cos\psi)|^2$ polynomial, (b) data for the 3^-, 9.64 MeV, state and a $|P_3(\cos\psi)|^2$ distribution, (c) and (d) E_x energy intervals 11.5–12 MeV and 12–13 MeV compared with the functions $|P_1(\cos\psi)|^2$ and $|P_3(\cos\psi)|^2$, respectively. (e) Excitation energy interval between the 9.64 and 10.84 MeV peaks. The data were projected onto the ψ axis at an angle that would correspond to a spin 2 state. The function shown is a corresponding $|P_2(\cos\psi)|^2$ Legendre polynomial.

once projected obliquely onto the ψ axis, in accordance with Eq. (3), produce a magnified angular range—see Ref. [14] for details.

The resulting angular distributions for the 10.84 MeV, 1^-, and 9.64 MeV, 3^-, states are shown in Figs. 5(a) and 5(b), respectively. The periodicity of the data is well matched by the appropriate order Legendre polynomial. Thus, the correlation analysis confirms the known spins of these states. Figure 5(e) shows the data that lie in a narrow region between the two peaks, close to 10 MeV. The angular correlations in this region appear to confirm the presence of the broad 10.3 MeV, 0^+, state, in that the gradient of the correlation ridges is equal to zero, as predicted by Eq. (3). Nevertheless, given that it is possible that there is a 2^+ state in this region the correlation data were projected at an angle that would correspond to $J = 2$. The projection is compared to a Legendre polynomial of order 2. It is clear that the polynomial and data have completely the wrong phase, and thus the $J = 2$ contribution to the data is small.

Finally, an inspection of the excitation energy region between 11 and 14 MeV (Fig. 5) indicates that the background level is much higher than above 14.5 MeV. This difference

may, in part, be due to broad ^{12}C excited states rather than background contaminants. To probe for such contributions the correlations were examined for the energy intervals $E_x = 11.5$–12 MeV and 12–13 MeV. These were found to be structured, with distributions indicative of spins 1 and 3, respectively [Figs. 5(c) and 5(d)]. The resulting angular distributions are shown compared with the polynomials of order 1 and 3. The fact that the data show structure that is similar to the other 1^- and 3^- states would indicate that there are indeed broad 1^- and 3^- resonances contributing to the background. We conclude that there is a broad 1^- resonance at $E_x \sim 11.8$ MeV and a broad 3^- resonance at $E_x \sim 12.5$ MeV.

Other portions of the excitation energy spectrum did not reveal such marked structure in the correlations. For example, above the 14.08 MeV state the correlations were largely featureless.

2. *Decays to* ^{8}Be(2^+)

The decay of the states in ^{12}C via the intermediate, ^{8}Be, 2^+ level was analyzed by recording the emission patterns in the center-of-mass frame of the ^{12}C nuclei. This was performed using the Dalitz parameters $\sqrt{3}(E_{1\mathrm{cm}} - E_{2\mathrm{cm}})/2$ and $(2E_{3\mathrm{cm}} - E_{1\mathrm{cm}} - E_{2\mathrm{cm}})/2$, where $E_{i\mathrm{cm}}$ is the center-of-mass energy of the i^{th} particle. A similar analysis for the 12.71 MeV, 1^+, state was performed in Ref. [15]. The spectra in Fig. 6 show the experimentally observed behavior for the 14.08 and 12.71 MeV states. The patterns displayed are clearly different for the two states and would be expected to depend strongly on the angular momenta governing the decay, the location, and the shape of the broad intermediate 2^+ resonance; the decay barriers (centrifugal and Coulomb); and the momentum phase-space available for the decay.

Figure 7 illustrates how the general behavior evolves as a function of the ^{12}C excitation energy. The circles drawn show the maximum displacement from the origin, which scales with excitation energies. The three bands indicate the locus of events associated with the decay through the ^{8}Be 2^+ state. The relative position of the bands changes with excitation energy, to the point where they form an intersection, star-like, pattern at 12.7 MeV. The different correlation patterns seen for the 14.08 and 12.71 MeV states can be seen to be strongly influenced by the different crossings of the ^{8}Be bands.

To reproduce the experimental signatures in detail a Monte Carlo simulation of the decay process was developed. This simulation generates the angular distributions of the three α particles based upon the correlation theory developed by Biedenharn and Rose [16]. For the decay of the 14.08 MeV, 4^+, state the orbital angular momenta of the $^8\mathrm{Be} + \alpha$ and $\alpha + \alpha$ systems are both $L = 2$ (assuming this dominates because of the lower barrier). The correlation theory produces an angular distribution, $W(\theta)$, for the emission of the α particle from the decay of ^{8}Be, measured with respect to the first α particle emitted from the decay of the ^{12}C excited state given by

$$W(\theta) = 1 + 0.408 P_2(\cos(\theta)) + 0.020 P_4(\cos(\theta)), \quad (4)$$

where P_2 and P_4 are Legendre polynomials of order 2 and 4, respectively. For the decay of the 1^+ state at 12.71 MeV the orbital angular momenta are again both $L = 2$, but due to the differing initial spin the correlation coefficients are modified, with the angular distribution being given by

$$W(\theta) = 1 + 0.714 P_2(\cos(\theta)) - 1.714 P_4(\cos(\theta)). \quad (5)$$

The sensitivity to the decay phase-space, width of the intermediate 2^+ state, and centrifugal and Coulomb barriers was included in the simulations. The distribution of energies with which the ^{8}Be intermediate state was populated was generated using the following form,

$$P(E_x(^8\mathrm{Be})) = \frac{P_l(^8\mathrm{Be} + \alpha) P_{l'}(\alpha + \alpha) \sqrt{E_x(^8\mathrm{Be}) + Q_\alpha} \sqrt{E_x(^{12}\mathrm{C}) - E_x(^8\mathrm{Be}) - E_{\mathrm{thresh}}}}{(E_x(^8\mathrm{Be}) - E_{\mathrm{res}})^2 - \Gamma_{\mathrm{res}}^2/4}, \quad (6)$$

where E_{res} and Γ_{res} are the centroid and width of the 2^+ resonance in ^{8}Be, i.e., 2.9 and 1.5 MeV. $P_l(^8\mathrm{Be} + \alpha)$ and $P_{l'}(\alpha + \alpha)$ are the energy-dependent penetrabilities calculated for the α decay of ^{12}C and ^{8}Be nuclei for orbital angular momenta l and l' and a channel radius of 1.4 fm. The two terms $\sqrt{E_x(^8Be) + Q_\alpha}$ and $\sqrt{E_x(^{12}C) - E_x(^8Be) - E_{\mathrm{thresh}}}$ account for the change in momentum phase-space with excitation energy of the two systems ($Q_\alpha = 0.093$ MeV and $E_{\mathrm{thresh}} = 7.365$ MeV). The denominator in Eq. (6) describes the resonance properties of the intermediate state and the numerator decay barriers and phase-space. In addition, the Monte Carlo simulations also include the experimental acceptances (energy and angular) and also the energy and angular resolution of the detectors.

Finally, in both the simulations and the experimental data, the ordering of the three α particles is randomized to remove any bias that is imposed because of the electronic ordering of the strips and detectors as they are processed by the data acquisition system (the spectra in Fig. 6 have had this randomization applied). To quantitatively compare the simulations with the experimental data the spectra in Fig. 6 were separated out into a radial and an angular part (just as was performed in Ref. [15]). It should be noted that both the radial and the angular dependence of these data explore the energy dependence of the decay process, but probe different facets of the energy correlations between the three α particles produced in the decay process.

In this analysis the data are plotted as a function of the distance from the origin, $\sqrt{3}(E_{1\mathrm{cm}} - E_{2\mathrm{cm}})/2 = (2E_{3\mathrm{cm}} - E_{1\mathrm{cm}} - E_{2\mathrm{cm}})/2 = 0$, and the angle,

$$\theta = \tan^{-1}((2E_{3\mathrm{cm}} - E_{1\mathrm{cm}} - E_{2\mathrm{cm}})/(\sqrt{3}(E_{1\mathrm{cm}} - E_{2\mathrm{cm}})). \quad (7)$$

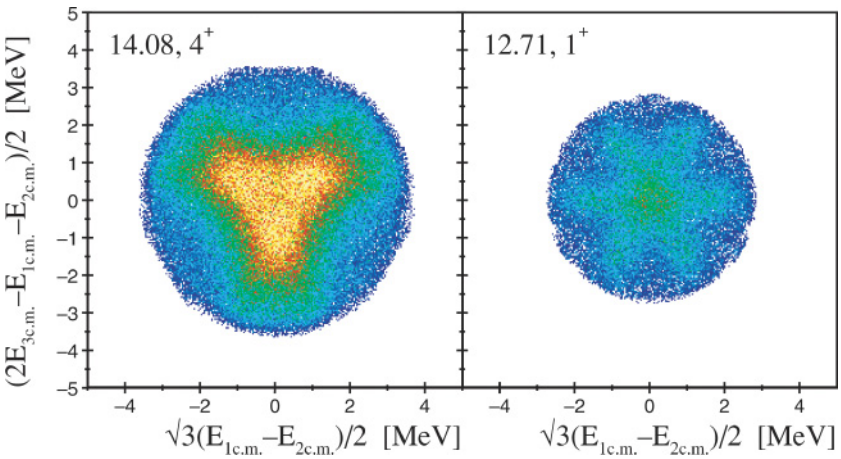

FIG. 6. (Color online) Dalitz plots for the decays of the 14.08 and 12.71 MeV states via the 2^+ excited state in ^{8}Be.

Figure 8 shows the experimental distributions for the 14.08 MeV state. The data are compared with two simulations, the first corresponds to the angular distributions generated in accordance with Eq. (4) and the second assumes an isotropic distribution, i.e., $W(\theta) = 1$. The angular dependence found in the simulations is only weakly dependent on the form of the correlation function, $W(\theta)$, and both provide a reasonable description of the data. The radial dependence is different in the two cases and appears to favor the isotropic form. The deviation from that predicted by Eq. (4) is not unexpected, because the correlation coefficients are appropriate only in the instance that the m-substate populations are also isotropic, as would be the case for instance in β decay. However, in this particular case it has been demonstrated (e.g., in Ref. [17]) that there is strong alignment in $^{12}\mathrm{C} + ^{12}\mathrm{C}$ inelastic scattering at these collision energies (we return to this point later). In principle, such correlation analysis could be used to extract the alignment. A similar analysis was performed for the 12.71 MeV, 1^+, state and is shown in Fig. 9. Again, the angular dependence of the data is well described by both the isotropic distribution and that described by Eq. (5). The radial dependence appears to lie somewhere between the two limiting cases.

It is apparent that the angular dependence is well described for the two states at 12.71 and 14.08 MeV and that the model provides a good description of the decay process. We now examine the distributions for the states at 11.83 and 13.35 MeV, both of which are assigned $J^\pi = 2^-$, the latter tentatively [12]. The unnatural parity of the states is clearly evident from the fact that they do not decay to the ^{8}Be ground state. Figure 10 shows the angular projection of the Dalitz plot for the 13.35 MeV state, employing a narrow gate around the peak region indicated in Fig. 4 (and hence the low statistics). It is clear from a comparison with the data in Figs. 8 and 9 that the structure present is not a result of feed-through from either the 12.71 or 14.08 MeV states (note the width of the structures is much larger than that for the 14.08 MeV state). The experimental spectrum is compared with simulations for decays of 2^-, 3^+, and 4^- unnatural parity states, where the orbital angular momenta for the first α decay are $L = 1$, 2, and 3, respectively. The expected isotropic contribution from the smooth background observed to underlie the peaks in Fig. 4 was added to the simulations at a level of 50%. The main difference between the three simulations is the depth of the minima between the double-peak maxima. The larger the $^{12}\mathrm{C} \rightarrow {}^8\mathrm{Be} + \alpha$ centrifugal barrier then the more pronounced

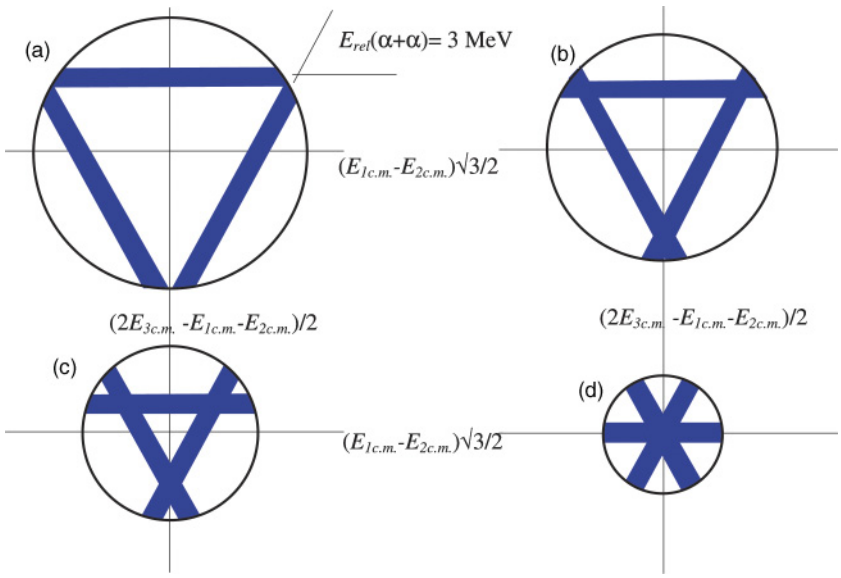

FIG. 7. (Color online) Illustration of the evolution of the Dalitz structure with ^{12}C excitation energy. The (blue) bands show the location of the ^{8}Be(2^+) resonance. Panel (a) corresponds to an excitation energy close to 20 MeV and panel (d) corresponds to an energy close to 12.7 MeV. Panels (b) and (c) correspond to energies of ~16 and ~14 MeV, respectively. The 12.71 MeV state corresponds to panel (d) and the 14.08 MeV state approximately to panel (c).

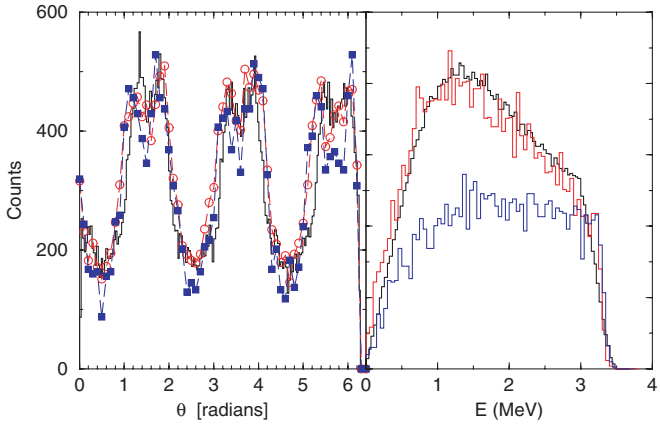

FIG. 8. (Color online) The angular (θ) and radial (E) dependence of the yield for the decay of the 14.08 MeV state corresponding to the data shown in Fig. 6 (black histogram). The simulations corresponding to the angular distributions described by Eq. (4) are shown by the (filled blue) squares and blue histogram, and the simulations assuming an isotropic distribution are shown by the (open red) circles and red histogram.

the minimum, which correlates with a greater localization of the decay strength in ^{8}Be (i.e., the range of excitation energies is decreased with higher centrifugal barrier). Because the patterns are very similar for all possible spin states a definitive spin assignment is not possible; however, it would appear more likely from the present analysis that the state has a spin and parity of either 3^{+} or 4^{-} (and more likely the latter), though in reality all states remain possible.

Figure 11 shows a similar analysis for the 11.83 MeV state. Once again, it can be determined that the influence of neighboring states on the oscillatory structure is small (i.e., the spectrum is substantially different from that for the 12.71 MeV state), but the analysis shown in Fig. 4 indicates

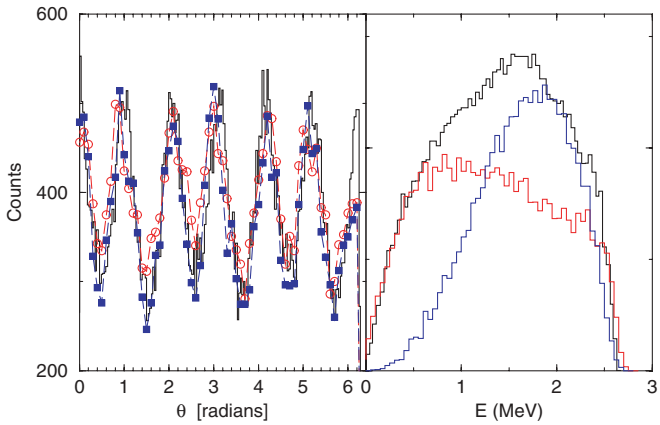

FIG. 9. (Color online) The angular dependence (θ) and radial (E) of the yield for the decay of the 12.71 MeV state corresponding to the data shown in Fig. 6 (black histogram). The simulations corresponding to the angular distributions described by Eq. (5) are shown by the (solid blue) squares and blue histogram, and the simulations assuming an isotropic distribution are shown by the (open red) circles and red histogram.

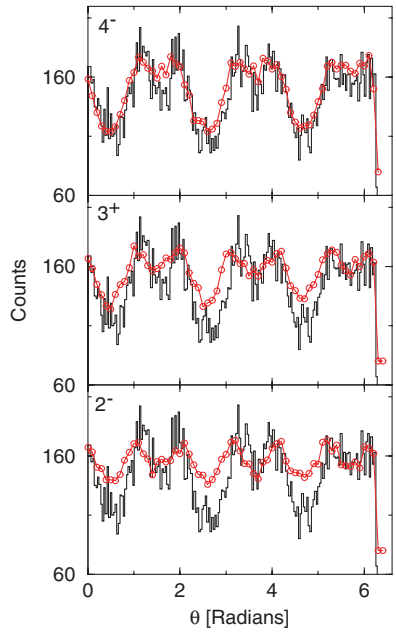

FIG. 10. (Color online) The angular dependence of the yield in the Dalitz analysis for the 13.35 MeV state, compared with the simulations (red open circles) for 2^{-}, 3^{+}, and 4^{-} decays. Note, it was assumed that there is a 50% contribution to the experimental spectrum from an isotropic background.

that the background contribution again could be as large as 50%. It should be noted that an analysis of the data between $E_x(^{12}\mathrm{C}) = 10$ and 11 MeV shows the background to be essentially flat. The experimental data for the 11.83 MeV

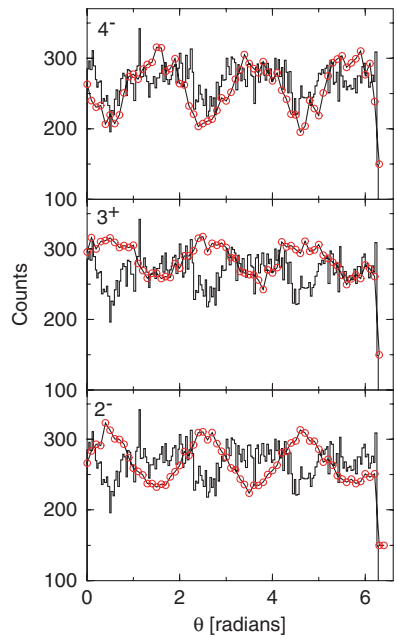

FIG. 11. (Color online) The angular dependence of the yield in the Dalitz analysis for the 11.83 MeV state, compared with the simulations (red open circles) for 2^{-}, 3^{+}, and 4^{-} decays. Note, it has been assumed that there is a 50% contribution to the experimental spectrum from an isotropic background.

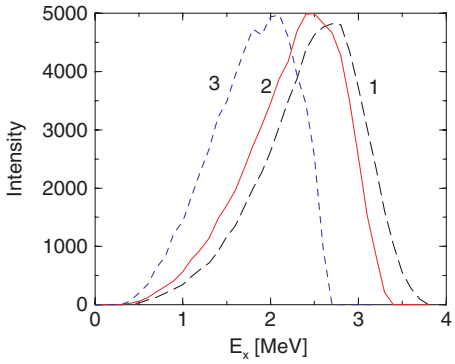

FIG. 12. (Color online) Calculated strength distribution functions for the decay of 2^- ($L = 1$), 3^+ ($L = 2$), and 4^- ($L = 3$) states to the tail of the 2^+ state in ^{8}Be. The higher the centrifugal barrier the greater the shift toward lower ^{8}Be excitation energies.

state are compared with three simulations for the 2^-, 3^+, and 4^- states. The simulations for 2^- decays and 3^+ decays are substantially similar, with just the depth of the minima being enhanced in the latter case. However, the phase of the oscillation pattern changes for the 4^- case. The 11.83 MeV state lies 4.47 MeV above the α-decay threshold, and thus for a $L = 0$ decay and considering the Coulomb barrier ($\sim$1.3 MeV) the decay to the low-energy half of the intermediate ^{8}Be, 2^+, state is permitted. However, for higher angular momenta decays the range of ^{8}Be excitation energies that are accessible is reduced. This is illustrated in Fig. 12, which shows the range of excitation energies in ^{8}Be produced in the simulations for the 2^-, 3^+, and 4^- decays ($L = 1$, 2, and 3). The larger barrier results in an enhanced feeding of the tail of the 2^+ state and a change in the correlation pattern. The present correlation analysis would indicate a larger decay barrier and thus a higher spin. Variations in the angular distribution function $W(\theta)$ for a 2^- decay cannot change the structure of the simulated results such that they reproduce the behavior observed in the experimental data. In fact, a rather large change in the $L = 1$ decay barrier (1 MeV) is required to reproduce the experimental data. In this way, the above conclusion appears to be rather robust.

IV. DISCUSSION

The present analysis provides evidence for the existence of the 11.16 MeV state reported in the ^{11}B(^{3}He,d) reaction and associated with an $l = 1$ transfer [18] and a 2^+ spin and parity. The state appears here only in the decay to the 2^+ state in ^{8}Be, which would be consistent with an absent centrifugal barrier. Alternatively, this may point to an unnatural parity state (i.e., 1^+ or 3^+) or a state with a high angular momentum. The angular distributions for the decay were isotropic (as expected for a 2^+ state); however, the background contribution was dominant, and thus no clear conclusion can be drawn. The β-decay measurements of Fynbo *et al.* [8] provide some guidance as to the possible character of the state. In the β decay of ^{12}N only positive parity states with spin 0, 1, or 2 may be strongly populated. There is no strong evidence for a 2^+ or a 1^+ state decaying via the 2^+ state in ^{8}Be in these measurements. Thus, it looks likely that the state is excluded from having $J^\pi = 0^+$, 1^+, and 2^+. This leaves possibly 3^+, or alternatively an incorrect determination of the transferred angular momentum from the analysis of the ^{11}B(^{3}He,d) reaction [18].

The 13.35 MeV state would appear to be confirmed as possessing unnatural parity due to the fact that it is not observed in the decay to the ^{8}Be ground state. At present it is tentatively assigned $J^\pi = 2^-$ [12]. This assignment is based upon a tentative $l = 0$ transfer extracted from a three-point angular distribution from the ^{11}B(^{3}He,d) reaction [18]. However, the data quality is such that they could equally correspond to $l = 1$ or 2 transfers. In the current analysis we cannot unambiguously determine the spin and parity, but the data indicate that an assignments of 3^+ or 4^- may be more appropriate (preferably the latter). It should be noted that the magnetic excitations of ^{12}C populated in electron inelastic scattering measurements were explored in Ref. [19]. These studies strongly indicated that the 13.35 MeV state was not the $M2$ excitation of a 2^- state and was more in line with a 4^- excitation.

Finally, there is the question as to the spin and parity of the 11.83 MeV state. The state is recorded in Ref. [12] as possessing spin and parity 2^-. The arrival at this assignment is interesting. Early measurements of the ^{11}B(^{3}He,d) reaction indicated very clearly an $l = 0$ transfer [20], and so it was recorded in Ref. [21] as possessing possible spins of 1^- or 2^-. The subsequent measurement of the same reaction at higher energy [18] indicated an $l = 2$ transfer (though this assignment cannot be considered unique). In later tabulations [12] the earlier $l = 0$ was dropped and a 2^- assignment adopted. A 1^- assignment has been argued for by a number of authors, for example, an analysis of decay correlations [22,23] or proton elastic scattering [24]. However, it is clear from the present studies that the state cannot have spin and parity 1^- because its decay characteristics are completely different from those of the 10.84 MeV 1^- state, which lies only 1 MeV lower in energy. The lack of any evidence for decay to the ground state of ^{8}Be suggests with high probability that the state does indeed have unnatural parity. The present decay spectrum (Fig. 11) for this state cannot be reproduced assuming centrifugal barriers associated with $L = 1$ or 2, but rather $L = 3$. If the angular momentum transfer, $l = 2$, asserted by Reynolds, Rundquist, and Poichar [18] is maintained, then this would be consistent with a 4^- state at 11.83 MeV rather than the presently adopted 2^-. Again the electron inelastic scattering measurements [19] found there were not in good agreement with the calculations for a 2^- state. The $M2$ calculations had to be scaled by 0.18 to reproduce the experimental data. An $M4$ distribution (corresponding to a 4^-) state has a magnitude closer to the data though the shape at lower momentum transfers may not be in such good agreement. What is abundantly clear is that more precise measurements are required for the ^{11}B(^{3}He,d) reaction, if the spectrum of states in this region is to be finally established.

A detailed understanding of the spectrum of states in ^{12}C above 7 MeV is a long-standing problem. For example, the nature of the 7.65 MeV state remains a subject of some debate [1–3], as does the location of any associated 2^+ state [7]. The 4^+ state at 14.08 MeV is known to be linked with the ground-state rotational band. According to antisymmetrized molecular dynamics (AMD) calculations [9], the 9.64 MeV, 3^-, state has a well-developed 3α cluster structure as does the 1^- state at 10.84 MeV. However, the shell-model calculations [6] also give such states in this region of excitation, whereas the 7.65 MeV, 0^+, state cannot be generated. In the cluster picture, there are rotational bands built on the 3^- and 1^- states that should have spin and parity 4^- and 2^-, respectively. It should be noted that the shell model gives states with these spins and parities in a similar excitation energy region also. From the cluster perspective, it is important to locate the lowest energy 4^- state in ^{12}C that would be associated with the $K^\pi = 3^-$ cluster band. The present measurements indicate that possible candidates for the 4^- state are the 11.83 and 13.35 MeV states. Given the ambiguity of the distributions for the 13.35 MeV state, it is possible that it possesses $J^\pi = 2^-$, in which case the 3^-–4^- pair of states would be 9.64 and 11.83 MeV, and the 1^-–2^- pair 10.84 and 13.35 MeV. The separations of these states are 2.2 and 2.5 MeV, respectively. The separation of the 1^-–2^- pair would be consistent with the shell model [6]. For a rotational band, the proposed separation of the 3^- and 4^- states would indicate a moment of inertia that is twice that of the ^{12}C ground state. For a constant moment of inertia, this would place the corresponding 5^- state close to 14.6 MeV. In the present measurements, this state would be expected to be smaller in amplitude than the lower spin states. Here, such an excitation would be partially masked by the relatively strong peak at 14.08 MeV. We note that a weak state is reported in the proton-transfer measurements of Hinds and Middleton [20] at 14.7 MeV.

V. SUMMARY AND CONCLUSIONS

An analysis of the α decay of ^{12}C excited states in the region 7–15 MeV was performed. The decay components to both the ^{8}Be ground and first excited state were separated and used to provide an indication of natural and unnatural parity states in this region. The distributions of the energies of the three α particles in the ^{12}C center-of-mass frame were used to gain insight into the spins of the states for the decay via the intermediate 2^+ state in ^{8}Be. In particular, we find evidence for the 11.16 MeV state seen earlier in the ^{11}B(^{3}He,d) reaction, and we suggest that the spin and parity of the 13.35 MeV state may be 2^-, 3^+, or 4^-, with it being more likely the higher spin state. An analysis of the decay of the 11.83 MeV state calls into question the 2^- assignment that has been *established* for this state. In addition, we find evidence for broad 1^- and 3^- resonances at $E_x \sim 11.8$ and $\sim$12.5 MeV, respectively.

These measurements demonstrate that our understanding of the structure of ^{12}C even at these moderate excitation energies requires further attention. In particular, detailed measurements of transfer reactions such as ^{11}B(^{3}He,d) are required to be certain of the character of these states.

ACKNOWLEDGMENTS

N. Ashwood and N. Curtis are thanked for careful reading of the manuscript, and H. Fynbo and W. Catford are thanked for their comments. The authors acknowledge the assistance of the Department of Nuclear Physics at the Australian National University (ANU) in running the experiments. The financial support of the U.K. Engineering and Physical Sciences Research Council (EPSRC) is acknowledged. The experimental work was performed under a formal agreement between the EPSRC and the ANU.

[1] A. Tohsaki, H. Horiuchi, P. Schuck, and G. Röpke, Phys. Rev. Lett. **87**, 192501 (2001).
[2] Y. Funaki, A. Tohsaki, H. Horiuchi, P. Schuck, and G. Röpke, Phys. Rev. C **67**, 051306(R) (2003).
[3] T. Yamada and P. Schuck, Phys. Rev. C **69**, 024309 (2004).
[4] W. von Oertzen, Eur. Phys. J. A **29**, 133 (2006).
[5] M. Chernykh, H. Feldmeier, T. Neff, P. von Neumann-Cosel, and A. Richter, Phys. Rev. Lett. **98**, 032501 (2007).
[6] P. Navrátil, J. P. Vary, and B. R. Barrett, Phys. Rev. Lett. **84**, 5728 (2000).
[7] M. Itoh *et al.*, Nucl. Phys. **A738**, 268 (2004); M. Itoh *et al.*, Mod. Phys. Lett. A **21**, 2359 (2006).
[8] H. O. U. Fynbo *et al.*, Nature **433**, 136 (2005).
[9] Y. Kanada-En'yo, Phys. Rev. Lett. **81**, 5291 (1998).
[10] R. L. Cowin and D. L. Watson, Nucl. Instrum. Methods A **399**, 365 (1997).
[11] C. A. Bremner *et al.*, Phys. Rev. C **66**, 034605 (2002).
[12] F. Azjenberg-Selove, Nucl. Phys. **A506**, 1 (1990).
[13] D. D. Caussyn, G. L. Gentry, J. A. Liendo, N. R. Fletcher, and J. F. Mateja, Phys. Rev. C **43**, 205 (1991).
[14] M. Freer, Nucl. Instrum. Methods A **383**, 463 (1996).
[15] H. O. U. Fynbo *et al.*, Phys. Rev. Lett. **91**, 082502 (2003).
[16] L. C. Biedenharn and M. E. Rose, Rev. Mod. Phys. **25**, 729 (1953).
[17] S. P. G. Chappell, W. D. M. Rae, C. A. Bremner, G. K. Dillon, D. L. Watson, B. Greenhalgh, R. L. Cowin, M. Freer, and S. M. Singer, Phys. Lett. **B444**, 260 (1998).
[18] G. M. Reynolds, D. E. Rundquist, and R. M. Poichar, Phys. Rev. C **3**, 442 (1971).
[19] R. S. Hicks, J. B. Flanz, R. A. Lindgren, G. A. Peterson, L. W. Fagg, and D. J. Millener, Phys. Rev. C **30**, 1 (1984).
[20] S. Hinds and R. Middleton, Proc. Phys. Soc. (London) **78**, 81 (1961).
[21] F. Azjenberg-Selove, Nucl. Phys. **A114**, 1 (1968).
[22] B. Antolkovic and J. Hudomalj, Nucl. Phys. **A237**, 253 (1975).
[23] B. Antolkovic and Z. Dolenec, Nucl. Phys. **A237**, 235 (1975).
[24] G. R. Satchler, Nucl. Phys. **A100**, 497 (1967).